Materials Letters 134 (2014) 306–310

Contents lists available at ScienceDirect

Materials Letters

journal homepage: www.elsevier.com/locate/matlet

Property optimization of porous metallic glasses via structural design

Baran Sarac [a,*], Jana Wilmers [a], Swantje Bargmann [a,b]

[a] Institute of Materials Research, Helmholtz-Zentrum Geesthacht, Max-Planck Straße 1, 21502 Geesthacht, Germany
[b] Institute of Continuum and Material Mechanics, Hamburg University of Technology, Eissendorfer Straße 42, 21073 Hamburg, Germany

ARTICLE INFO

Article history:
Received 20 June 2014
Accepted 11 July 2014
Available online 21 July 2014

Keywords:
Metallic glass
Microstructure
Stochastic design
Damage tolerance
Porous materials
Toughening mechanism

ABSTRACT

Systematization of material parameters is essential for property optimization. In this work, a gradient-extended continuum mechanical model implemented into a finite element code is utilized to analyze the influence of pore hierarchy on the overall mechanical response of porous metallic glasses. A spectrum of samples with randomized (stochastic) pore designs is comparatively studied with their periodic counterparts. It is shown that the pore design as well as the volume fraction has a strong effect on the mechanical response of the porous metallic glass structures. The results underline design aspects for certain applications.

1. Introduction

Metallic glasses constitute an important research focus due to their unique mechanical properties. To exemplify, very high yield strength close to the theoretical limit and large elastic strain at room temperature are typical properties of these advanced alloys. However, limited plasticity due to their amorphous nature creates a serious bottleneck for the applicability of monolithic metallic glasses. To overcome this drawback, several approaches to create metallic glass foams have been pursued. The foams can remarkably toughen the glass by forming localized shear bands through energy dissipation within the matrix [1–3]. Sarac et al. [4,5] address the influence of pores on the mechanical properties of bulk metallic glasses by a novel microstructure design strategy experimentally and numerically. In these studies, samples of various pore sizes, spacings, configurations and porosities were examined under uniaxial compression or tension, where periodic pore design facilitated for quantitative analyses.

The design criterion of advanced structures depends on customers' needs and application field, which is strongly correlated with optimization of one or several material parameters. Particularly for the optimization of mechanical properties, one must always consider the tradeoffs which significantly alter the performance of the final product. For example, it has recently been shown that high elastic energy storage during in-plane compression is observed by a geometric effect through pore configuration [6,7]. To improve the overall plasticity and toughness, a more effective stress transfer method during deformation is generated by the reconfiguration of microstructure. For example, nature-inspired metallic glass structures such as three dimensional scaffolds with random packing of foams [8] and two-dimensional cellular structures with stochastic patterns [9] revealed the high resistance of porous structures against localized deformation and fracture with relatively minor sacrifice on the yield strength.

Despite the high reliability of experimental data, time and financial investments to optimize the technical performance of advanced materials steer material's community towards numerical simulations [5]. Within this work, the model of Bargmann et al. [10] is used to investigate the effect of damage tolerance on the deformation characteristics of $Zr_{35}Ti_{30}Cu_{7.5}Be_{27.5}$ metallic glass under uniaxial in-plane compression for a range of stochastic micropore designs of different porosities. Furthermore, performance evaluation of these structures is comparatively conducted with the structures containing periodic pores.

2. Mathematical modeling and implementation

The rate-dependent, gradient-extended model is formulated thermodynamically consistently in the framework of continuum mechanics, and is based on the Helmholtz free energy and dissipation potential provided in [10,11]. Our model accounts for free volume generation and plastic slip and, thereby, maps size effects, shear localization and tension–compression asymmetry (for a model with similar characteristics see also [12]). The highly nonlinear and strongly coupled governing equations are solved by a dual mixed finite element algorithm [13]. Displacement controlled

* Corresponding author. Tel.: +49 15165167851.
E-mail addresses: b.sarac@ifw-dresden.de (B. Sarac), swantje.bargmann@tuhh.de (S. Bargmann).

http://dx.doi.org/10.1016/j.matlet.2014.07.064

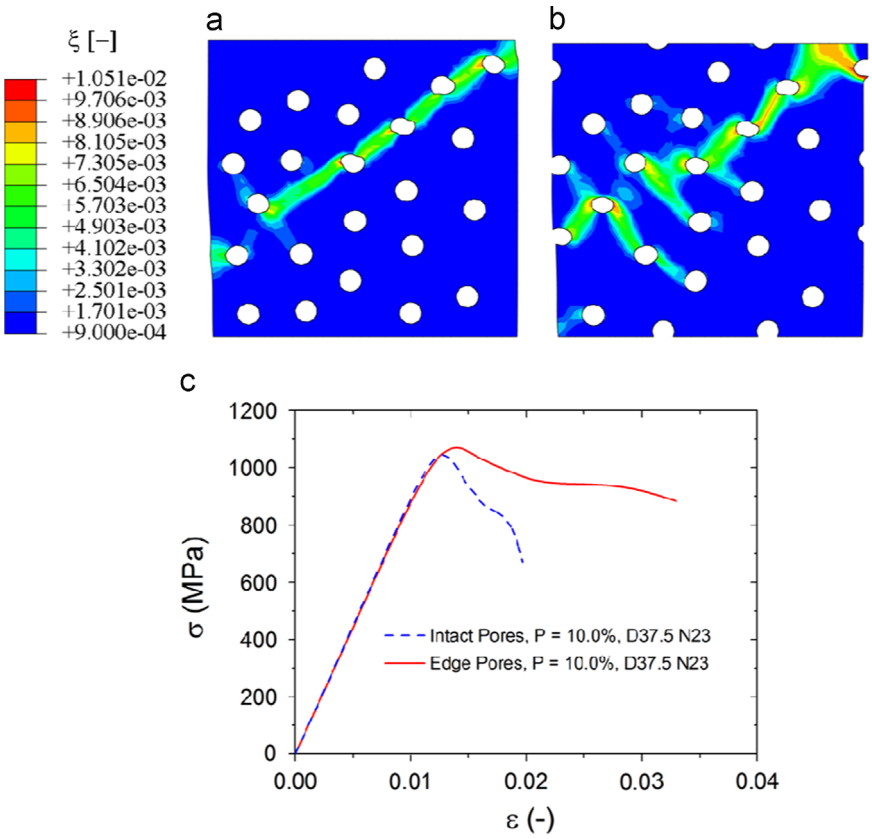

Fig. 1. Influence of edge pores on the mechanical response. Class I sample with porosity $P=10\%$, diameter of pores $D=37.5$ μm, and number of pores $N=23$. (a) Sample with intact edges. This type of design is affected by shear localization. Shear branching is prevailed by the free volume localization effect particularly caused by the free volume accumulation on the edges. (b) Similar sample of the same porosity and minimum spacing, but with edge pores, showing shear branching throughout the deformation. (c) Samples with edge pores display enhanced overall deformation behavior. Our studies have shown that this behavior also holds for other pore designs with different porosities.

uniaxial compression is applied at the nodal points of the top face at a macroscopic strain rate of 0.005 s^{-1}. The nodal points at the bottom face of the squares are fixed in *x*- and *y*- directions. In addition, micro-free boundary conditions are assumed, i.e., the free volume gradient vanishes in normal direction at all boundaries. The numerical analyses are performed on 2D square specimens (500 μm × 500 μm). Material parameters used for the implementation of the model are adopted from [5]. Samples are discretized into between 2000 and 3000 plane-strain elements depending on the pore design. Mesh-independent deformation behavior is observed due to gradient dependence of the model. Calculations are done in ABAQUS via the UELEMENT interface, and an ABAQUS python script was utilized for post-processing.

3. Micropore design

Previous studies emphasized the importance of using circular pores stacked in AB pattern within the metallic glass matrix, by which the elastic and plastic deformation can be remarkably enhanced [4,5]. Thus, reference samples of different porosities from periodic pattern are generated to compare with samples having stochastic design.

The source code for the generation of stochastic pore design is programmed in C++ and compiled using Visual Studio. For determining the pore positions, a standard pseudo-random number generator is used. A minimum distance between pores is included within the code to prevent overlap and is manually adjusted as a function of radius (or average radii) of the pores depending on the design criteria. The samples generated are periodic at the boundaries to analyze the effect of the exact number of pores and the corresponding porosity on the mechanical behavior. For the sake of simplicity in analysis, a maximum of two different pore sizes is used. For the sets of samples with a single pore size (stochastic class I), a maximum number of pores permitted by the minimum spacing criteria is selected to increase the influence of pores on stress localization. Further, samples with two different pore sizes (stochastic class II) are designed in a way that the total porosity becomes 10.0%, 20.0% or 30.0% (± 0.2% standard deviation), where contributions of pore size and number of pores are investigated in comparison with stochastic class I and periodic class structures with single pore size. Pore diameters of 37.5 μm and 50 μm are chosen for stochastic class II samples to analyze the contribution of a different pore size on the overall response. Each sample set comprises average values of the mechanical properties of three or more samples to increase the accuracy of the data.

An additional constraint of minimum spacing has to be established, if the side pores overlapping with the boundaries are to be eliminated. This arrangement limits the random distribution of pores, which in return alters the deformation behavior (see Fig. 1 and Video 1). Localized shear zones at an angle perpendicular to the loading are generated for a 10.0% porosity sample which decreases the entire performance of the structure (Fig. 1a). Thus, in the following, structures with edge pores are selected due to their higher mechanical properties caused by shear branching (Fig. 1b, and dark yellow squares in Figs. 3–5).

Supplementary data associated with this article can be found in the online version at 10.1016/j.jmps.2010.09.009.

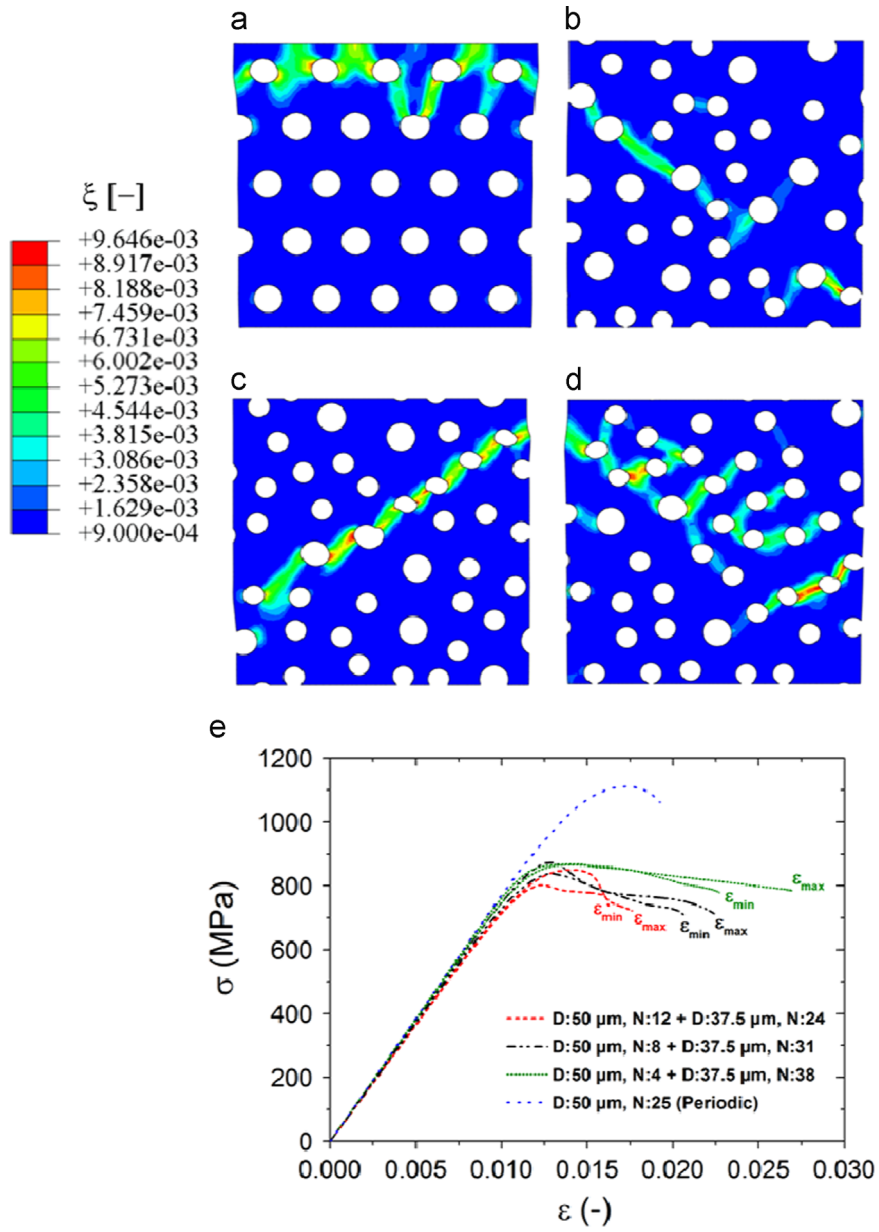

Fig. 2. Influence of pore design on the mechanical behavior at a constant porosity of 20.0%. (a–d) Free volume distribution; (e) stress–strain responses. (a) Sample with AB periodic pore configuration. Pore diameter and spacing: 50 μm. (b–d) Stochastic pore distributions comprised of two different pore sizes. The contour plots for (b) and (c), indicated by the red and black curves in (e), respectively, show localized shear zones between the pores at an angle of ~40°, whereas the contour plot for (d), indicated by the green curve in (e), exhibits widely scattered shear zones. (e) Stress–strain data of various pore designs. The findings show that the dissipation of the free volume is favored below a certain critical ratio φ which enhances the mechanical properties (see green curve). *D*: diameter of pores, *N*: number of pores, and ε_{max} and ε_{min}: maximum and minimum final strain (for various stochastic distributions) selected for each design criteria. (For interpretation of the references to color in this figure legend, the reader is referred to the web version of this article.)

4. Results and discussion

High free volume generation within the samples is known to be the cause of plastic shear in metallic glasses [14–16]. Thus, we study its distribution to investigate the shear zone formation and development. Fig. 2 and Video 2 show the spatial free volume distribution of 20.0% porosity samples before fracture takes place. For samples with periodic pore designs, deformation is highly accumulated around the edges of the specimen (Fig. 2a). Yield strength and ultimate compressive strength of these samples (which are defined for metallic glasses as the 0.2% offset point from the linear-elastic region [17] and the onset point of shear zone localization [5], respectively) are higher compared to that of the stochastic pore designs at the expense of final strain.

Supplementary data associated with this article can be found in the online version at 10.1016/j.matlet.2014.07.064.

For 20.0% samples, the findings highlight the influence of the ratio of number of bigger-sized to smaller-sized pores φ within the same sample. If the ratio φ is large (red and black curves in Fig. 2e), shear is localized at an angle to the loading direction along which the resultant shear stress becomes minimum (Fig. 2b and c). For the stochastic class II samples having smaller φ ratio (green curves in Fig. 2e), the free volume is disseminated evenly within the samples, which results in higher plasticity and damage tolerance at no expense of compressive strength (Fig. 2d).

Comparison of the ultimate compressive strengths of the samples is provided in Fig. 3. The change in ultimate strength follows a linear trend for all classes of pore designs. For the considered porosity

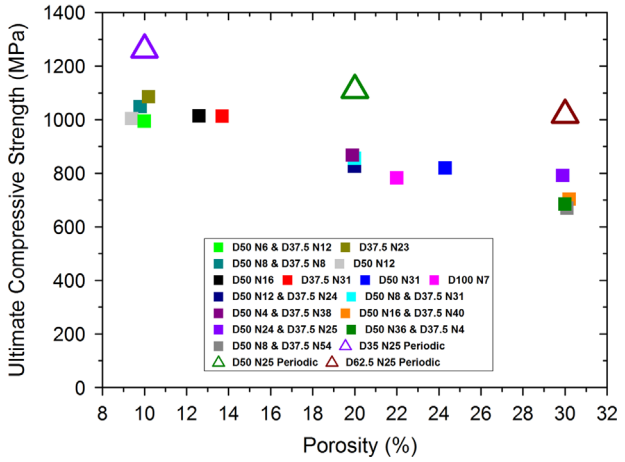

Fig. 3. Ultimate compressive strengths of different pore designs as a function of porosity (D: pore diameter and N: number of pores). Class I samples contain a single pore size (e.g., diameter $D=37.5$ μm, and number of pores $N=23$, indicated by dark yellow square), whereas class II samples contain two different pore sizes (e.g., 4 pores with diameter $D=50$ μm and 38 pores with diameter $D=37.5$ μm, indicated by purple square). Class III samples with periodic pore design (e.g., 25 pores with diameter $D=35$ μm indicated by violet triangle) surpasses the other pore classes of interest for the analyzed region. (For interpretation of the references to color in this figure legend, the reader is referred to the web version of this article.)

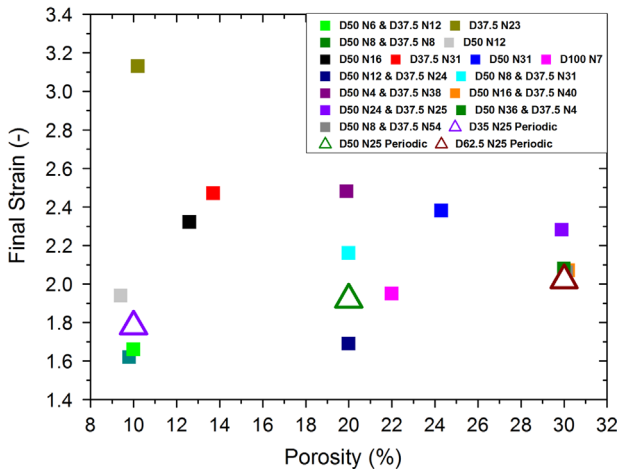

Fig. 4. Fracture strains of different pore designs as a function of porosity (D: pore diameter and N: number of pores). Class I sample with 23 pores of diameter 37.5 μm (dark yellow square) and class II sample with 4 pores of diameter 50 μm and 38 pores of diameter 37.5 μm (purple square) show the ultimate final strain for the porosities of 10.0% and 20.0%, respectively. (For interpretation of the references to color in this figure legend, the reader is referred to the web version of this article.)

range, samples with periodic pore designs show higher strengths compared to that of the stochastic pore designs. This can be attributed to the symmetric and homogeneous free volume and stress distribution until reaching the ultimate strength. The ultimate strength of metallic glasses is in general very high. Hence, depending on the customers' needs, a certain decrease in it can be affordable.

To observe the influence of pore design over macroscopic plasticity, fracture strains captured by the adopted model are considered in Fig. 4. The best performance is obtained from the stochastic class I sample containing 23 pores with diameters of 37.5 μm (dark yellow square), showing average final strain of 3.13%. In general, class I pore designs display higher final strain compared to the other classes if porosity is chosen below 15.0%. If the porosity is selected between 20.0% and 25.0%, both classes I and II samples generally exhibit higher plasticity than the periodic

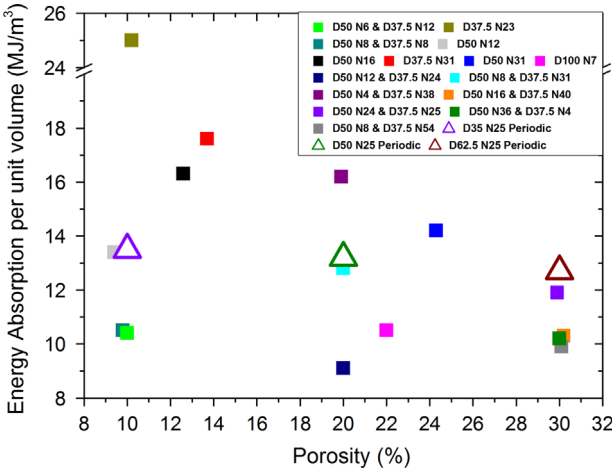

Fig. 5. Energy absorption per unit volume of the considered pore designs calculated from the areas under the stress–strain curves (D: pore diameter and N: number of pores). Class I sample with 23 pores of diameter 37.5 μm (dark yellow square) and class II sample with 4 pores of diameter 50 μm and 38 pores of diameter 37.5 μm (purple square) show the highest energy absorption per unit volume for the porosities of 10.0% and 20.0%, respectively. (For interpretation of the references to color in this figure legend, the reader is referred to the web version of this article.)

design. Among these, the class II sample with 4 pores of diameter 50.0 μm and 38 pores of diameter 37.5 μm (purple square) has 2.48% final strain. Plasticity difference between the sample classes is subtle as the porosity becomes ~30.0%, where class II design with similar number of pores of different sizes (D: 50.0 μm, N: 24 and D: 37.5 μm, N: 25, violet square) shows relatively higher fracture strain. Therefore, for 30.0% porosity, optimized properties are achieved if the ratio $\varphi \sim 1$.

Fig. 5 depicts the energy absorption comparison of different class samples. Again, class I sample with 23 pores of diameter 37.5 μm (dark yellow square) outperforms all the other designs, and shows around 85.0% higher energy absorption compared to its periodic counterpart of the same porosity. For 20.0% porosity, class II sample with 4 pores of diameter 50 μm and 38 pores of diameter 37.5 μm (purple square) reveals 30.0% higher energy absorption than that of the periodic class design, where the branching of the free volume within the sample is the indicative of this enhanced behavior (see Fig. 2d). For relatively high porosities of ~30%, the deformation pattern becomes independent of the pore design. This means that the stress accumulations in the near vicinity of pores are playing a critical role for an earlier catastrophic failure [5].

5. Conclusions

This paper focuses on the design and selection criteria of porous metallic glasses. Compared to experimental methods, the gradient-extended numerical approach in this study provides a faster and more effective way of analyzing complex stochastic patterns. The findings show that particularly below 25.0% porosity, enhanced plasticity and energy absorption can be attained with the stochastic pore design. Among the ultimate values, 1.5 and 2 times higher energy absorption is obtained for the 10.0% porosity sample compared to its 20.0% and 30.0% porosity counterparts, respectively (Fig. 5). Homogeneous distribution of shear zones within metallic glass samples is verified to be an extremely effective toughening mechanism which is reflected in the high damage tolerance of stochastic pore designs. In contrast, if the yield/ultimate strength or elastic energy is of higher significance for the specific application, periodic design with AB pore stacking along with smaller porosity

should be the designer's first choice. Finally, the effect of the additional constraint through intact edge pore design is found to be noteworthy, and needs to be considered during the design stage of the structure. Overall, the design criteria presented in this study can be directly applicable to foams, and to some extent to composites.

References

[1] Schroers J, Veazey C, Johnson WL. Appl Phys Lett 2003;82:370–2.
[2] Wada T, Inoue A, Greer AL. Appl Phys Lett 2005;86:251907.
[3] Brothers AH, Dunand DC. Adv Mater 2005;17:484–6.
[4] Sarac B, Schroers J. Nat Commun 2013;4:1–7.
[5] Sarac B, Klusemann B, Xiao T, Bargmann S. Acta Mater 2014;77:411–22.
[6] Sarac B, Ketkaew J, Popnoe DO, Schroers J. Adv Funct Mater 2012;22:3161–9.
[7] Sarac B, Schroers J. Scr Mater 2013;68:921–4.
[8] Demetriou MD, Veazey C, Harmon JS, Schramm JP, Johnson WL. Phys Rev Lett 2008;101:1–4.
[9] Chen W, Liu Z, Robinson HM, Schroers J. Acta Mater 2014;73:259–74.
[10] Bargmann S, Xiao T, Klusemann B. Philos Mag 2014;94:1–19.
[11] Klusemann B, Bargmann S. J Mech Behav Mater 2013;22:51–66.
[12] Thamburaja P. J Mech Phys Solids 2011;59:1552–75.
[13] Bargmann S, Ekh M, Runesson K, Svendsen B. Philos Mag 2010;90:1263–88.
[14] Spaepen F. Acta Metall Mater 1977;25:407–15.
[15] Argon AS. Acta Metall Mater 1979;27:47–58.
[16] Srolovitz D, Vitek V, Egami T. Acta Metall Mater 1983;31:335–52.
[17] Fan C, Ott RT, Hufnagel TC. Appl Phys Lett 2002;81:1020–2.